
P. SRITONWONG,¹ S. SANORPIM,^{1,2} K. ONABE³

¹ Nanoscience and Technology, Graduate School, Chulalongkorn University
(Bangkok 10330, Thailand; e-mail: phosrphai@gmail.com)

² Department of Physics, Faculty of Science, Chulalongkorn University
(Bangkok 10330, Thailand)

³ Department of Advanced Materials Science, The University of Tokyo
(Kashiwanoha, Kashiwa, Chiba 277-8561, Japan)

STRUCTURAL PROPERTIES OF LATTICE-MATCHED InGaPN ON GaAs (001)

UDC 539

Structural properties of lattice-matched InGaPN on GaAs (001) have comprehensively investigated by high resolution X-ray diffraction (HRXRD), Raman spectroscopy, and atomic force microscopy (AFM). The InGaPN layers were grown by metal organics vapor phase epitaxy (MOVPE). To obtain the lattice-matched InGaPN on GaAs, flow rates of trimethylindium (TMIn), trimethylgallium (TMGa) were kept, respectively, at 14.7 and 8.6 $\mu\text{mol}/\text{min}$. On the other hand, the N content optimized by varying the flow rate of dimethylhydrazine (DMHy, N precursor) was controlled at 300 $\mu\text{mol}/\text{min}$. With a combination of HRXRD and Raman scattering measurements, the In and N contents are estimated to be 55.8 and 0.9 at%, respectively. The lattice-mismatch lower than 0.47%, which corresponds to the lattice-matching condition, was confirmed for all the layers. The rapid thermal annealing (RTA) process was performed to improvement the crystalline quality of InGaPN layers. The annealing temperature was fixed at 650° C, which is an optimum growth temperature of a GaAs buffer layer. The annealing time was varied in a range of 30 to 180 s to verify a composition uniformity. With increasing the annealing time up to 120 s, the In and N contents were slightly increased. The AFM-root mean square (RMS) roughness of the InGaPN surface was observed to be reduced. For higher annealing times, the N content was dramatically reduced, whereas the In content was still remained. Moreover, the RMS roughness was observed to be increased. RTA at 650° C for 120 s demonstrated a significant improvement of structural properties of the lattice-matched InGaPN layers on GaAs (001).

Keywords: InGaPN, RTA, HRXRD, MOVPE, Raman scattering.

1. Introduction

InGaPN is an interesting dilute nitride due to the tunable structural and optical properties. Its lattice constant can be lattice-matched to various substrates such as GaAs [1, 2] and GaP [3, 4], by adjusting the indium (In) and nitrogen (N) contents. A huge bowing parameter, which is a characteristic of the dilute III-V-nitrides, can cause a large reduction of

the bandgap with a small amount of the N incorporation [4, 5]. On the other hand, these tunable properties, both the lattice constant and bandgap, make InGaPN to be suitable in many applications such as a multi-junction solar cells [1, 2], light emitting diodes (LEDs) [1, 6, 7], lasers, and heterojunction bipolar transistors [1, 2].

For the ternary and quaternary dilute nitride semiconductors, it is known that the structural properties can be greatly improved by the rapid thermal

annealing (RTA) at temperatures higher than the growth temperature [5–7]. In this work, to verify the structural properties of InGaPN layers grown on GaAs (001), the as-grown layer and annealed layers are investigated by high-resolution X-ray diffraction (HRXRD), Raman spectroscopy, and atomic force microscopy (AFM). The structural properties such as the lattice-mismatch, alloy composition, strain, and surface roughness are addressed to demonstrate the RTA-induced improvement of the crystalline quality of InGaPN layers.

2. Experimental Details

InGaPN layers were grown on GaAs (001) substrates by metalorganic vapor phase epitaxy (MOVPE). Trimethylgallium (TMGa), trimethylindium (TMIn), tertiarybutylphosphine (TBP), tertiarybutylamine (TBAs), and dimethylhydrazine (DMHy) were used as precursors of Ga, In, P, As, and N, respectively. The pressure and total flow rate were, respectively, kept at 60 Torr and 2000 sccm during the growth. Before the InGaPN growth, the GaAs substrate was thermally cleaned at 650 °C in the TBAs atmosphere for 15 min. A 100-nm-thick GaAs buffer layer was grown at 650 °C for 10 min. The growth temperature and growth time of InGaPN were 520 °C and 10 min, respectively. To obtain the [TMIn]/([TMIn] + [TMGa]) mole fraction of 0.63, the flow rates of TMIn and TMGa were, respectively, kept at 14.7 and 8.6 $\mu\text{mol}/\text{min}$ for all the layers. We note that the [TMIn]/([TMIn] + [TMGa]) mole fraction of 0.63 is expected to make the compressive strain in the InGaPN grown layer. The N content was controlled by the DMHy flow rate taken to be 300 $\mu\text{mol}/\text{min}$. To improve the layer quality, the post-growth rapid thermal annealing (RTA) treatments were performed with various annealing times. The samples were cut into the four small parts. The annealing temperatures was kept at 650 °C, which is an optimum growth temperature of a GaAs buffer layer, with a halogen lamp in the N₂ ambient. The annealing time was 30, 60, 120, and 180 s. Moreover, during RTA, the GaAs wafer was used to cover the InGaPN surface to prevent any desorption of the group-V elements. All the grown layers were morphologically characterized by AFM to obtain the surface feature and root mean square (RMS) roughness. The Raman scattering measurement was performed to verify the In content. The

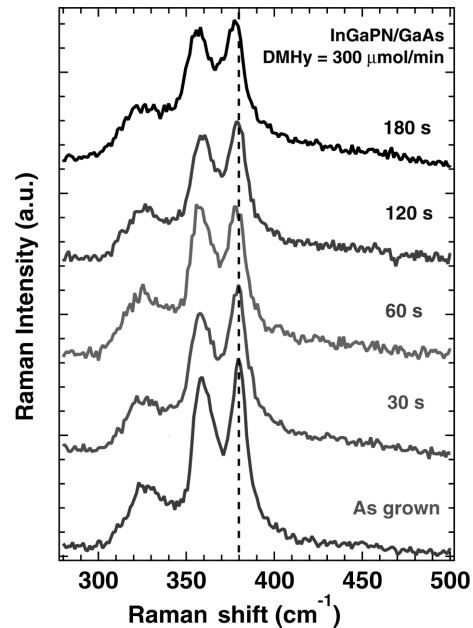


Fig. 1. Raman spectra of the InGaPN alloy films with a DMHy flow rate of 300 $\mu\text{mol}/\text{min}$. The different annealing times were applied to as-grown layer and those annealed at 30, 60, 120, and 180 s at the annealing temperature 650 °C

514.5-nm line of an Ar⁺ laser with excitation spot of about 2 μm was used as a Raman excitation source. Based on HRXRD measurements, both a symmetric (004) $2\theta/\omega$ -scan and an asymmetric (115) reciprocal space maps (RSMs) were constructed to investigate both normal (a_{\perp}) and in-plane (a_{\parallel}) lattice parameters. With a combination of Raman scattering and HRXRD measurements [8], an alloy composition and a lattice-mismatch in InGaPN on GaAs (001) were examined as a function of the annealing time.

3. Results and Discussion

Figure 1 illustrates the Raman spectra of an as-grown InGaPN layer on GaAs (001) substrates as well as the layers annealed with different annealing times: 30, 60, 120, and 180 s. The Raman spectra consist of three features located at wave numbers of 380, 360, and 330 cm^{-1} , which are attributed to GaP-like LO, InP-like LO, and InP-like TO phonon modes, respectively. These three peaks are observed for all the InGaPN layers. Similar spectra for as-grown and post-growth rapid thermal annealed layers were observed. The peak position of the GaP-Like

Relaxed lattice constant (a_0), lattice-mismatches and In content determined by micro-Raman spectroscopy, and N content calculated for the DMHy flow rate of 300 $\mu\text{mol}/\text{min}$

Annealing time, s	GaP-LO, cm^{-1}	a_n , A°	a_p , A°	a_0 , A°	Lattice mismatched, %	In, %	N, %
0	378.7 ± 0.5	5.70	5.66	5.68	0.47	55.8 ± 0.8	0.9 ± 0.4
30	378.4 ± 0.5	5.69	5.67	5.68	0.41	56.2 ± 0.8	0.9 ± 0.4
60	377.2 ± 0.6	5.70	5.65	5.68	0.39	58.2 ± 0.8	2.0 ± 0.4
120	377.2 ± 0.6	5.69	5.65	5.67	0.33	58.2 ± 0.8	2.4 ± 0.4
180	377.0 ± 0.6	5.70	5.67	5.68	0.54	58.5 ± 0.8	1.2 ± 0.4

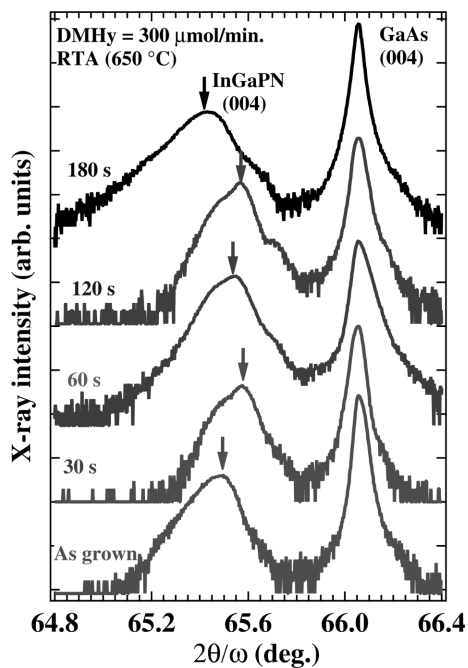


Fig. 2. HRXRD (004) $2\theta/\omega$ curves of InGaPN alloy films grown on GaAs (001) substrates with the DMHy flow rate of 300 $\mu\text{mol}/\text{min}$. The annealing times for the as-grown and annealed layers were 30, 60, 120, and 180 s at the annealing temperature 650 $^\circ\text{C}$

LO phonon mode shows a slightly shift from $378.7 \pm 0.5 \text{ cm}^{-1}$ for the as-grown layer to $377.2 \pm 0.6 \text{ cm}^{-1}$ for the layer annealed for 180 s. The peak positions of the GaP-Like LO phonon mode of all layers are listed in Table. It is known that the In content in InGaP is significantly related to the optical phonon frequencies, especially the GaP-like LO phonon reported by Bedel *et al.* [9]. A shift of the GaP-like LO phonon frequency ($\Delta\omega_{\text{GaP-likeLO}}$) as a function of the In content (x) is expressed as

$$\Delta\omega_{(\text{GaP-likeLO})} = -18.18x^2 - 38.97x.$$

Here, ($\Delta\omega_{\text{GaP-likeLO}}$) is a difference between the frequencies of the GaP-like LO phonon mode taken from InGaP compared to that of the GaP-LO phonon mode (404.99 cm^{-1}) taken from GaP. It is found that the variation of the In content is $\pm 1.7 \text{ at.}\%$ from HRXRD, whereas the value of $\pm 0.8 \text{ at.}\%$ was determined from Raman scattering. This uncertainty represents an error, which is introduced by a step size in the wave-number axis. According to the GaP-like LO phonon frequencies, $\omega_{\text{GaP-likeLO}}$, the In content in InGaPN layers was determined to be 55.8 ± 0.8 and 56.2 ± 0.8 , 58.2 ± 0.9 , 58.2 ± 1.1 , and $58.5 \pm 1.1 \text{ at.}\%$ for the as-grown and annealed layers for 30, 60, 120, and 180 s, respectively. An increase of the In content due to the RTA treatment can be described by a reorganization of In atoms in the InGaPN layer from the interstitial sites to the lattice site. Thus, the In atoms obtain the thermal energy from the RTA process to rearrange their positions.

Figure 2 shows HRXRD (004) $2\theta/\omega$ profiles for the InGaPN layers, both as-grown and annealed layers with different annealing times of 30, 60, 120, and 180 s. The diffraction pattern, which consists of a well-defined diffraction peak located at 66.06° and a broad curve at lower diffraction angles, looks similar for both the as-grown and annealed layers. The diffraction peak located at 66.06° is referred to the GaAs (004) reflection, while the diffraction peak located at a lower angle indicates the InGaPN (004) reflection. Compared to the as-grown layer, the InGaPN (004) reflection peak is shifted to higher angles with increasing the annealing time up to 120 s. On the other hand, for the annealing time of 180 s, the InGaPN (004) reflection peak is shifted back to lower angles. The peak shift of the InGaPN (004) reflection is resulted from the alloy composition change due to the RTA treatment. In fact, an increase of the In and N contents in the InGaPN layer exhibits a shift of

the InGaPN (004) reflection peak to lower angles and higher angles, respectively. Thus, the peak shifts of the InGaPN (004) reflection are mainly caused by an increase of the N content. According to the Raman scattering results, the In content was increased by the RTA treatment. Therefore, the annealed layers with the annealing time up to 120 s exhibited an increase of the N content. In this case, the diffraction peak shifts to higher angles. In contrast, a decrease of the N content was found for the annealing time of 180 s, leading to a peak position lowering.

Figure 3 shows HRXRD reciprocal space maps (RSMs) taken around an asymmetric (115) reflection for the InGaPN films on GaAs (001), which are illustrated for the as-grown layer (a) and the annealed layers with the annealing times of (b) 120 and (c) 180 s. It is seen that the diffraction from the InGaPN (115) planes is clearly observed for both the as-grown and annealed layers. When the annealing time increases up to 120 s, the diffraction contour of InGaPN (115) reflection shows the orientation along the full strained line indicated by the dashed line, as shown in Fig. 3, (b). This moving trend indicates that more N content is incorporated into the layers. However, for the annealing time of 180 s, the InGaPN (115) contour shifts back away from the fully strained line, which causes the InGaPN layer to become a partially strained layer. With the use of the In content calculated by a shift of the GaP-like LO phonon and the normal (a_{\perp}) and in-plane (a_{\parallel}) lattice parameters obtained from HRXRD measurements, the N content in the InGaPN layers can be evaluated by the modified Vegard law [10, 11],

$$a_{\text{InGaPN}} = \frac{2C_{12}a_{\parallel} + C_{12}a_{\perp}}{2C_{12} + C_{11}}, \quad (1)$$

$$a_{\text{InGaPN}} = (1-x)[(1-y)a_{\text{GaP}} + ya_{\text{GaN}}] + x[(1-y)a_{\text{InP}} + ya_{\text{InN}}], \quad (2)$$

$$C_{11} = \frac{(1-x)(1-y)a_{\text{GaP}}C_{11}^{\text{GaP}} + ya_{\text{GaN}}C_{11}^{\text{GaN}}}{a_{\text{InGaPN}}} + \frac{x[(1-y)a_{\text{InP}}C_{11}^{\text{InP}} + ya_{\text{InN}}C_{11}^{\text{InN}}]}{a_{\text{InGaPN}}}, \quad (3)$$

$$C_{12} = \frac{(1-x)(1-y)a_{\text{GaP}}C_{12}^{\text{GaP}} + ya_{\text{GaN}}C_{12}^{\text{GaN}}}{a_{\text{InGaPN}}} + \frac{x[(1-y)a_{\text{InP}}C_{12}^{\text{InP}} + ya_{\text{InN}}C_{12}^{\text{InN}}]}{a_{\text{InGaPN}}}, \quad (4)$$

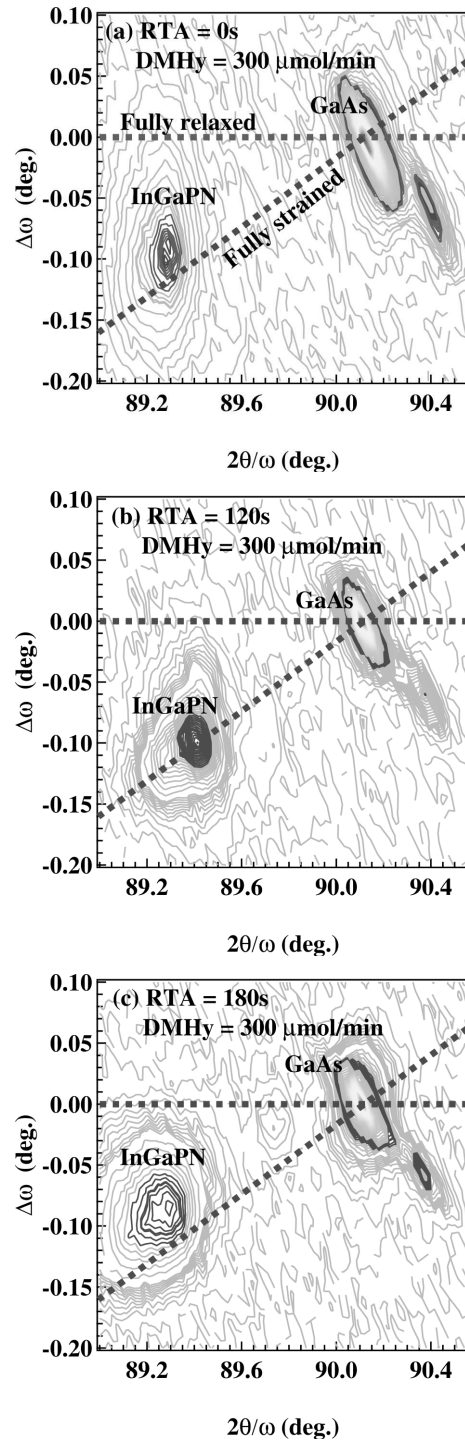


Fig. 3. HRXRD $2\theta/\omega$ reciprocal space maps around an asymmetric (115) reflection for the InGaPN films on GaAs (001) for the DMHy flow rate $300 \mu\text{mol}/\text{min}$ for the as-grown layer (a) and with the annealing times of 120 (b) and 180 s (c) at 650°C

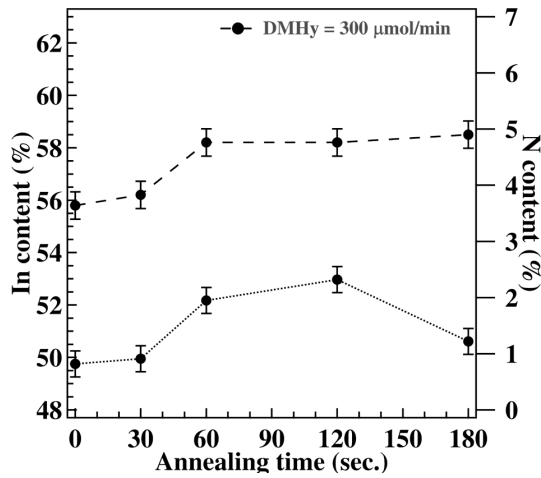


Fig. 4. In and N contents as functions of the annealing time for InGaPN alloy films

where C_{11} and C_{12} are the elastic constants $In_xGa_{1-x}P_{1-y}N_y$ and a_{GaP} , a_{GaN} , a_{InP} , and a_{InN} are the relaxed lattice constants of cubic GaN, GaP, InP, and cubic InN, respectively. Since the elastic constants of $In_xGa_{1-x}P_{1-y}N_y$ are not available, they can, thus, be derived from the elastic constants of the four binary compounds, by using the interpolation method. Thus, the In and N contents in the InGaPN alloy layer were determined. The list of alloy compositions of the as-grown and annealed InGaPN layers with different annealing times is given in Table.

Figure 4 shows the N and In contents dependent on the annealing time. The N content is increased, when the annealing time increase up to 120 s. The highest N content is $2.4 \pm 0.4\%$. Furthermore, the reduction of the N content to $1.2 \pm 0.4\%$ is observed, when the annealing time increases up to 180 s. To explain the results, it is proposed that the RTA treatment may induce the diffusion of both the In and N atoms inside the InGaPN layer. The lattice-mismatch is found to decrease, when we increase the annealing time up to 120 s. The lowest lattice-mismatch was observed to be 0.33%, which is smaller as compared to that of the as-grown layer equal to 0.47%. Unfortunately, the highest lattice-mismatch of 0.54% is found for the annealing time of 180 s. The lattice-matching condition between the layer and the substrate prevents the epitaxial layer from a misfit dislocation, which degrades the crystalline quality of the grown layer. Thus, the annealing effect causes a change in the alloy composition, both the In and N contents and in the strain

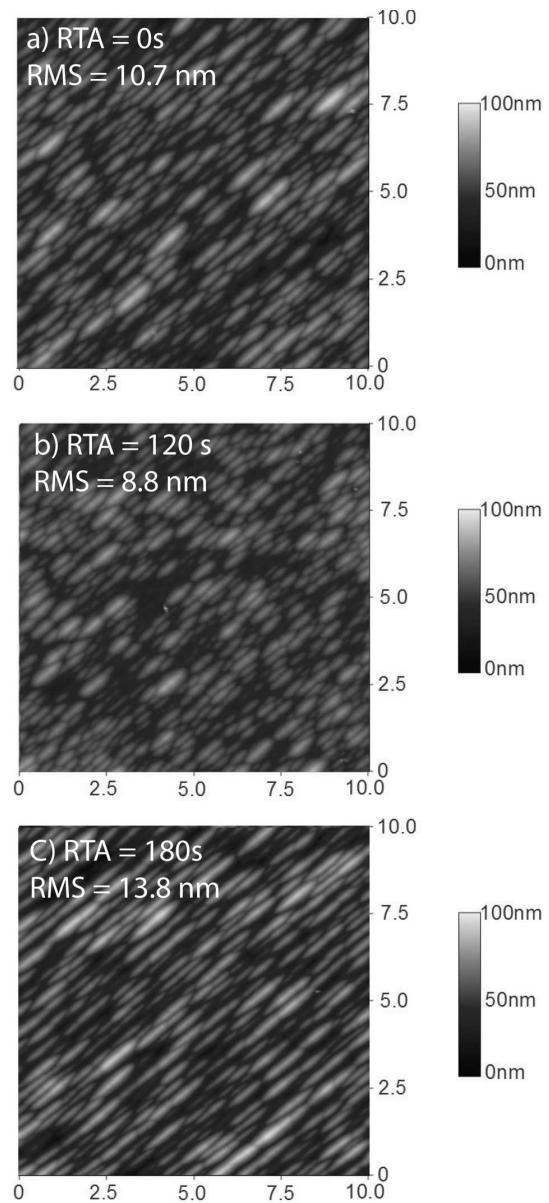


Fig. 5. AFM images of the InGaPN alloy films with the flow rate of DMHy of $300 \mu\text{mol}/\text{min}$ with annealing time for the as-grown layer (a) and the layers annealed for 120 (b) and 180 s (c) at 650°C

in the InGaPN layer. As a result, the post-growth RTA process shows a significant impact to improve the structural properties of the InGaPN layer.

The surface AFM images of five InGaPN layers are shown in Fig. 5. The scanning area is $10 \times 10 \mu\text{m}$. The elliptic island-like structure, which is elongated along

the [110] direction, was observed for all layers. A cross-hatch pattern due to the generation of a misfit dislocation is not observed. The root-mean-square (RMS) roughness of the layer surface is reduced from 10.7 to 8.8 nm, when the annealing time was increased up to 120 s. The result implies that the atom at the surface gains the thermal energy from the annealing process to re-arrange the own position by the mass transportation at the surface. However, when the annealing time increase from 120 s to 180 s, the RMS roughness is dramatically increased to 13.8 nm. This indicates that a longer annealing time causes a formation of the atom changing from 2D layer to a 3D mound. Combined with HRXRD results, these results demonstrate an evidence of the reduction in the misfit dislocation, as the annealing time increases to 120 s at 650 °C. Based on our results, the InGaPN layer annealed for 120 s at 650 °C exhibits the highest In and N incorporation in InGaPN, which are $58.2 \pm 0.8\%$ and $2.4 \pm 0.4\%$, respectively. The lowest RMS roughness of the layer surface was observed to be 8.8 nm. The lowest lattice-mismatch of 0.33% was obtained. These results suggest that the suitable selection of the annealing time helps to improve the structural properties of InGaPN.

4. Summary

Structural properties of InGaPN on GaAs (001) are investigated to verify the influence of the RTA treatment on the lattice-mismatch, alloy composition, strain, and surface morphology, which are studied by Raman spectroscopy, HRXRD measurements, and AFM. RTA at 650 °C for 120 s demonstrates a modification of the structural properties of the lattice-matched InGaPN layers on GaAs (001). A lowering of lattice-mismatch as small as 0.33% is confirmed. The RMS roughness of the InGaPN surface was decreased to the smallest value of 8.8 nm. The In and N contents were observed to be increased. With increasing the annealing time from 120 s to 180 s, the lattice-mismatch and RMS roughness were observed to be increased. The N content was dramatically reduced due to a desorption of N atoms from the surface, while the In content was remained. Our results suggest the RTA-induced rearrangement of the In and N atoms to improve structural properties of the lattice-matched InGaPN layer on GaAs (001) substrate.

This research has been supported by the Ratchadaphiseksomphot Endowment Fund of Chulalongkorn University (RES560530229-EN) and the 90th Anniversary of Chulalongkorn University Fund (the Ratchadaphiseksomphot Endowment Fund).

1. D. Kaewket, S. Sanorpim, S. Tungasmita, R. Katayama, K. Onabe. MOVPE growth of high optical quality InGaPN layers on GaAs (001) substrates. *Phys. Status Solidi C* **7**, 2079 (2010).
2. Y.G. Hong, R. André, C.W. Tu. Gas-source molecular beam epitaxy of GaInNP/GaAs and a study of its band lineup. *J. Vac. Sci. Technol B* **19**, 1413 (2001).
3. K. Onabe, T. Kimura, N. Nakadan, J. Wu, Y. Ito, S. Yoshida, J. Kikawa, Y. Shiraki. In: *The Thirteenth International Conference on Crystal Growth in Conjunction with the Eleventh International Conference on Vapor Growth and Epitaxy (ICCG-13/ICVGE-11)*, Kyoto (2001).
4. D. Kaewket, S. Tungasmita, S. Sanorpim, R. Katayama, K. Onabe. InGaPN/GaP lattice-matched single quantum wells on GaP (001) grown by MOVPE. *Adv. Mater. Res.* **55–57**, 821 (2008).
5. C.W. Tu, W.M. Chen, I.A. Buyanova, J.S. Hwang. Material properties of dilute nitrides: Ga(In)NAs and Ga(In)NP. *J. Cryst. Growth* **288**, 7 (2006).
6. H.P. Xin, R.J. Weltry, Y.G. Hong, C.W. Tu. Gas-source MBE growth of Ga(In)NP/GaP structures and their applications for red light-emitting diodes. *J. Cryst. Growth* **227–228**, 558 (2001).
7. V.A. Odnoblyudov, C.W. Tu. Growth and fabrication of InGaNP-based yellow-red light emitting diodes. *Appl. Phys. Lett* **89**, 191107 (2006).
8. P. Sritonwong, S. Sanorpim, K. Onabe. Composition investigations of nearly lattice-matched InGaPN films on GaAs (001) substrates grown by MOVPE. *Chaing Mai J. Sci.* **43** (2), 288 (2016).
9. E. Bedel, R. Carles, A. Zwick, J.B. Renucci, M.A. Renucci. Selectivity of resonant Raman scattering in $\text{InAs}_x\text{P}_{1-x}$ solid solutions. *Phys. Rev. B* **30**, 5923 (1984).
10. S. Sanorpim, F. Nakajima, N. Nakandan, T. Kimura, R. Katayama, K. Onabe. MOVPE growth and optical investigations of InGaPN alloys. *J. Cryst. Growth* **275**, e1017 (2005).
11. T.S. Wang, K.I. Lin, J.S. Hwang. Characteristics of InGaPN/GaAs heterostructures investigated by photoreflectance spectroscopy. *J. Appl. Phys.* **100**, 093709 (2006).
12. H. Lee, D. Biswas, M.V. Klein, H. Morkoc, D.E. Aspnes. Study of strain and disorder of $\text{In}_x\text{Ga}_{1-x}\text{P}/(\text{GaAs}, \text{graded GaP})$ ($0.25 \leq x \leq 0.8$) using spectroscopic ellipsometry and Raman spectroscopy. *J. Appl. Phys.* **75**, 5040 (1994).
13. K.I. Lin, J.Y. Lee, T.S. Wang, S.H. Hsu, J.S. Hwang, V. Hong, C.W. Tu. Effects of weak ordering of InGaPN. *Appl. Phys. Lett.* **86**, 211914 (2005).

14. N.V. Besslov, T.T. Dedegkrev, A.N. Efimov, N.F. Karntenko, YuP. Yakovlev. *Sov. Phys. Solid State* (English Transl.), **22**, 1652 (1980).
15. D.D. Sell, H.C. Casey, K.W. Wecht. Concentration dependence of the refractive index for *n*- and *p*-type GaAs between 1.2 and 1.8 eV. *J. Appl. Phys.* **45**, 2650 (1974).
16. G. Giesecke, H. Pfister. Präzisionsbestimmung der gitterkonstanten von $A^{III}B^V$ -verbindungen. *Acta Crystallogr.* **11**, 369 (1958).
17. M. Bugajski, W.J. Lewandowski. Concentration-dependent absorption and photoluminescence of *n*-type InP. *J. Appl. Phys.* **57**, 521 (1985).
18. D. Kaewket, S. Sanorpim, S. Tungasmita, R. Katayama, K. Onabe. Band alignment of lattice-matched InGaPN/GaAs and GaAs/InGaPN quantum wells grown by MOVPE. *Physica E* **42**, 1176 (2010).
19. M.E. Sherwin, T.J. Drummond. Predicted elastic constants and critical layer thicknesses for cubic phase AlN, GaN, and InN on β -SiC. *J. Appl. Phys.* **69**, 8423 (1991).
20. P.E. Jahne, W. Giehler, L. Hildish. Non-isodisplacement of P atoms in long-wavelength optical phonons in $In_{1-x}Ga_xP$. *Phys. Status Solidi B* **91**, 155 (1979).
21. K.M. Kim, S. Nonoguchi, D. Krishnamurthy, S. Emura, S. Hasegawa, H. Asahi. Optical properties of InGaPN epilayer with low nitrogen content grown by molecular beam epitaxy. *J. Appl. Phys.* **12**, 063507 (2012).
22. S.F. Yoon, K.W. Mah, H.Q. Zheng, B.P. Gay, P.H. Zhang. Observation of weak ordering effects and surface morphology study of InGaP grown by solid source molecular beam epitaxy. *Microelectronics J.* **31**, 15 (2000).

Received 27.12.17

П. Сритонвонг, С. Санорпін, К. Онабе

СТРУКТУРНІ ВЛАСТИВОСТІ InGaPN НА GaAs (001), УЗГОДЖЕНІ ЗА ПАРАМЕТРОМ ҐРАТКИ

Резюме

Досліджено властивості структури InGaPN на GaAs (001), узгоджені за параметром ґратки, із застосуванням рентгівської дифракції високої роздільної здатності (РДВРЗ), Раманівської спектроскопії (РС) і атомної силової мікроскопії (АСМ). Шари InGaPN були вирощені методом епітаксії металоорганічних з'єднань з газової фази. При отриманні InGaPN, узгодженого за параметром ґратки, на GaAs швидкості потоків тріметиліндія і тріметилгалія були, відповідно, 14,7 та 8,6 мкмоль/хв. Зміст N було оптимізовано при швидкості потоку диметилгідрозина (попередник N), що дорівнює 300 мкмоль/хв. Комбінуючи РДВРЗ і РС вимірювання, зміст In і N оцінено як 55,8 і 0,9 ат.%, відповідно. Для всіх шарів неузгодженість ґратки була менше 0,47%. Для поліпшення якості ґратки InGaPN шарів, застосований швидкий термічний відпал (ШТВ) при температурі 650 °C, оптимальної для зростання GaAs буферного шару. Час відпалу змінювався від 30 до 180 с для досягнення однорідності складу. Збільшення часу відпалу до 120 с призвело до незначного зростання змісту In і N. При цьому АСМ показала, що середньоквадратична шорсткість InGaPN поверхні зменшилася. При збільшенні часу відпалу різко падає вміст N без змін у вмісті In. Середньоквадратична шорсткість також зростає. ШТВ при 650 °C протягом 120 с значно поліпшив властивості структури шарів InGaPN на GaAs (001), узгоджених за параметром ґратки.